RAC1 induces nuclear alterations through the LINC complex to enhance melanoma invasiveness

Paula Colón-Bolea[a], Rocío García-Gómez[a,b], Sue Shackleton[c], Piero Crespo[a,b], Xosé R. Bustelo[b,d], and Berta Casar[a,b,*]

[a]Instituto de Biomedicina y Biotecnología de Cantabria, Consejo Superior de Investigaciones Científicas (CSIC), Universidad de Cantabria, Santander 39011, Spain; [c]Department of Biochemistry, University of Leicester, Leicester LE1 9HM, UK; [b]Centro de Investigación Biomédica en Red de Cáncer (CIBERONC), Instituto de Salud Carlos III, Madrid 28029, Spain; [d]Centro de Investigación del Cáncer and Instituto de Biología Molecular y Celular del Cáncer (CSIC), Universidad de Salamanca, Salamanca 37007, Spain

ABSTRACT **RHO GTPases are key regulators of the cytoskeletal architecture, which impact a broad range of biological processes in malignant cells including motility, invasion, and metastasis, thereby affecting tumor progression. One of the constraints during cell migration is the diameter of the pores through which cells pass. In this respect, the size and shape of the nucleus pose a major limitation. Therefore, enhanced nuclear plasticity can promote cell migration. Nuclear morphology is determined in part through the cytoskeleton, which connects to the nucleoskeleton through the Linker of Nucleoskeleton and Cytoskeleton (LINC) complex. Here, we unravel the role of RAC1 as an orchestrator of nuclear morphology in melanoma cells. We demonstrate that activated RAC1 promotes nuclear alterations through its effector PAK1 and the tubulin cytoskeleton, thereby enhancing migration and intravasation of melanoma cells. Disruption of the LINC complex prevented RAC1-induced nuclear alterations and the invasive properties of melanoma cells. Thus, RAC1 induces nuclear morphology alterations through microtubules and the LINC complex to promote an invasive phenotype in melanoma cells.**

Monitoring Editor
Peter Van Haastert
University of Groningin

Received: Feb 24, 2020
Revised: Sep 23, 2020
Accepted: Sep 28, 2020

INTRODUCTION

RHO GTPases are key regulators of cellular functions such as cytoskeletal regulation, cellular anchorage, cell motility, and migration, all essential processes for cancer progression and metastatic dissemination (Vega and Ridley, 2008; Bid *et al.*, 2013; Moshfegh *et al.*, 2014; Maldonado and Dharmawardhane, 2018). Among RHO GTPases, RAC isoforms display a significant mutational rate in some tumors. Indeed, The Cancer Genome Atlas (TCGA) data show that RAC is up-regulated or mutationally activated in over 10% of human cancers, including glioblastoma, melanoma, bladder, skin, esophageal, gastric, head and neck, liver, pancreatic, prostate, and uterine carcinomas (Kazanietz and Caloca, 2017). In particular, the driver mutation P29S appears in a significant proportion of melanomas and breast cancer cases (Krauthammer *et al.*, 2012; Davis *et al.*, 2013). Likewise, deregulation of upstream regulators such as the exchange factors Dbl, Vav, Trio, T-cell invasion and metastasis gene product (Tiam-1), epithelial cell transforming gene 2 (Ect2), and phosphatidylinositol-3,4,5-trisphosphate (PIP3)-dependent Rac exchange factor 1 (P-Rex-1) also contribute to aberrant RHO GTPases activity in a substantial number of tumors (Lindsay *et al.*, 2011; Wertheimer *et al.*, 2012; Cook *et al.*, 2014).

Nuclear atypia, abnormal nuclear morphology, is frequently observed in tumors, in many cases associated with an unfavorable prognosis (Erhardt *et al.*, 1989; Takeshima *et al.*, 1998). Recent

This article was published online ahead of print in MBoC in Press (http://www.molbiolcell.org/cgi/doi/10.1091/mbc.E20-02-0127) on October 7, 2020.

Competing interests: The authors declare no competing interests.

Authors contributions: P.C.B. and R.G.G. performed most of the experiments; P.C.B., R.G.G., and B.C. also prepared the figures and performed the statistical analyses; X.R.B. and S.S. designed experiments, interpreted the data, and provided key expertise; P.C. and B.C. conceived the study, directed it, analyzed and interpreted data, and wrote and corrected the manuscript.

*Address correspondence to: Berta Casar (casarb@unican.es).

Abbreviations used: BSA, bovine serum albumin; CAM, chorioallantoic membrane; FBS, fetal bovine serum; LINC, Linker of Nucleoskeleton and Cytoskeleton; SRE, serum response element; TBS, Tris-buffered saline.

evidence indicates that nuclear plasticity is a critical factor in cell migration, as nuclear size and shape constitute the limiting factor in allowing cells to squeeze through small spaces (Wolf *et al.,* 2013). In this respect, the connection between the nucleus and the cytoskeleton is critical for the transmission of the force necessary to drive nuclear deformation (Starr *et al.,* 2001; Zhang *et al.,* 2009; Lombardi *et al.,* 2011). The Linker of Nucleoskeleton and Cytoskeleton complex (LINC), composed of KASH and SUN proteins, connects the nucleus to cytoskeletal filaments and performs diverse functions including nuclear positioning and mechanotransduction (Chang *et al.,* 2015). The importance of this connection is reflected in the fact that mutations in the proteins that participate in this union contribute to diseases such as muscular dystrophy of Emery-Dreifuss, ataxia, progeria, and multiple tumors (Chen *et al.,* 2012; Luxton and Starr, 2014).

As master regulators of the cytoskeleton (Hall and Nobes, 2000; Abreu-Blanco *et al.,* 2014), it is therefore conceivable that RHO GTPases should play a major role in the regulation of nuclear shape. The findings reported herein support a model in which RAC1, among other RHO GTPases, acts as a key orchestrator of nuclear morphology by a process dependent on the tubulin cytoskeleton and LINC complex integrity to promote an invasive phenotype in melanoma cells.

RESULTS

RHO GTPases induce alterations in nuclear morphology in melanoma cells

To gain an initial insight into the participation of RHO GTPases in nuclear shape control in melanoma cells, we investigated whether the overexpression of constitutively active, GTP-bound (QL) mutant forms had an effect on nuclear morphology. To precisely score those cells expressing the GTPases, these were fused to GFP. In all melanoma cell lines tested, the three GTPases under study, RAC1, RHOA, and CDC42, elicited nuclear alterations, although the proportion of affected nuclei was higher in those cells overexpressing RAC1 or CDC42 (Figure 1a).

To study this phenomenon in further depth, we established a classification of the nuclei based on the morphologies resulting from the overexpression of the GTPases: rounded (normal), kidney shaped, multinucleated, multilobed, elongated, and doughnut (Figure 1b) and scored the emergence of these nuclear morphologies depending on the GTPase. Forty percent of A375p cells expressing activated RHO exhibited nuclear abnormalities. This proportion rose to nearly 60% in the case of RAC1 and CDC42. Kidney shaped was the most abundant nuclear aberration in cells overexpressing activated RAC1 and RHO, whereas CDC42 yielded mainly multinucleated cells. Thus, although RAC1 and CDC42 elicited a similar proportion of aberrant nuclei, the resulting nuclear morphologies were different. Furthermore, in cells overexpressing the active GTPases, we observed nuclear phenotypes that almost never appeared in control cells, such as elongated and doughnut-shaped nuclei (Figure 1c). To demonstrate that nuclear changes were a consequence of the activation, not of the overexpression, of the RHO GTPases, we performed the same experiment but using dominant inhibitory mutant forms of the GTPases, constitutively bound to GDP. In this case, no significant nuclear alterations were detected in any case (Supplemental Figure S1). These results demonstrated that the ectopic expression of constitutively active forms of RHO GTPases can bring about marked alterations in nuclear morphology.

To investigate whether the activation of the endogenous GTPases could also elicit nuclear alterations, we expressed an oncogenic form of the exchange factor Vav2, a bona fide activator of RAC1, RHO, and CDC42 (Abe *et al.,* 2000; Liu and Burridge, 2000). Remarkably, onco-Vav2 overexpression evoked nuclear alterations that mostly resembled those resulting from the overexpression of Rac1QL, with the greatest proportion corresponding to kidney-shaped nuclei and to a lesser extent multiple and multilobed nuclei (Figure 1d). As further proof of the effect of physiological RAC1 activation on nuclear morphology, we analyzed nuclear pleomorphism in IGR-1 melanoma cells that endogenously express RAC1 harboring the P29S mutation, which causes the constitutive activity of the GTPase and promotes melanocyte proliferation and migration (Davis *et al.,* 2013). When comparing these to A375p cells overexpressing RAC1Q61L, we found similar numbers of nuclei with an altered morphology (Figure 1e), although in the case of IGR-1 cells, the number of multilobed nuclei was greater than in A375p-RAC1QL. Overall, these results demonstrated that hyperactivity of RHO GTPases, particularly RAC1, induces profound alterations in nuclear morphology.

Alterations in nuclear morphology are independent of RHO GTPases-evoked gene expression

We wanted to clarify whether the effect of RHO GTPases on nuclear morphology was being exerted directly from the cytoplasm through mechanical effects or, rather, it was a consequence of transcriptional programs switched on by the GTPases. To this end, the import of proteins into the nucleus was prevented by the expression of RAN Q69L (Steggerda and Paschal, 2002), thereby preventing the nuclear entry of transcription factors that have been activated by the GTPases. It was observed that the pattern of nuclear pleomorphism evoked by the RHO GTPases was largely unaltered in the presence of RANQL, with the exception of a minor increase in kidney-shaped cells in cells expressing CDC42QL (Figure 2a). Conversely, RANQ69L markedly reduced the activity of a luciferase reporter under the control of a serum response element (SRE; Figure 2b) known to respond transcriptionally to RHO GTPases stimulation (Posern and Treisman, 2006; Busche *et al.,* 2008; Croft and Olson, 2011). To further study this point, we assessed by qPCR the transcriptional status of the RAC1-dependent SRF/MRTF transcription program in A375p cells overexpressing RAC1Q61L and RANQ69L. Recently it has been described that active RAC1 activates SRF/MRTF transcription program in melanocytes (Lionarons *et al.,* 2019); however, we did not found transcriptional changes in these genes in A375p cells harboring BRAFV600E mutation when overexpressing RAC1Q61L and RANQ69L (Supplemental Figure S2).

Therefore, these results allowed us to conclude that the ability of RHO GTPases to induce alterations in nuclear morphology is independent of their role in gene regulation.

RAC1QL alters nuclear morphology through the actin and tubulin cytoskeletons

Consequently, we decided to analyze whether RAC1 was evoking nuclear deformation through the cytoskeleton. To this end we treated cells with nocodazole, which blocks tubulin polymerization, thereby preventing the assembly of microtubules (Vasquez *et al.,* 1997). In this case, the proportion of cells displaying nuclear abnormalities in cells expressing RAC1Q61L was dramatically diminished, particularly those with kidney-shaped nuclei, and the distribution of the different nuclear morphologies was very similar to that of control cells (Figure 3a). Likewise, we tested if the acto-myosin cytoskeleton was involved in RAC-induced nuclear deformation by treating cells with cytochalasin D and blebbistatin (Straight *et al.,* 2003; Atilla-Gokcumen *et al.,* 2010). By contrast, in these cases the total number of abnormal nuclei resulting from these treatments was

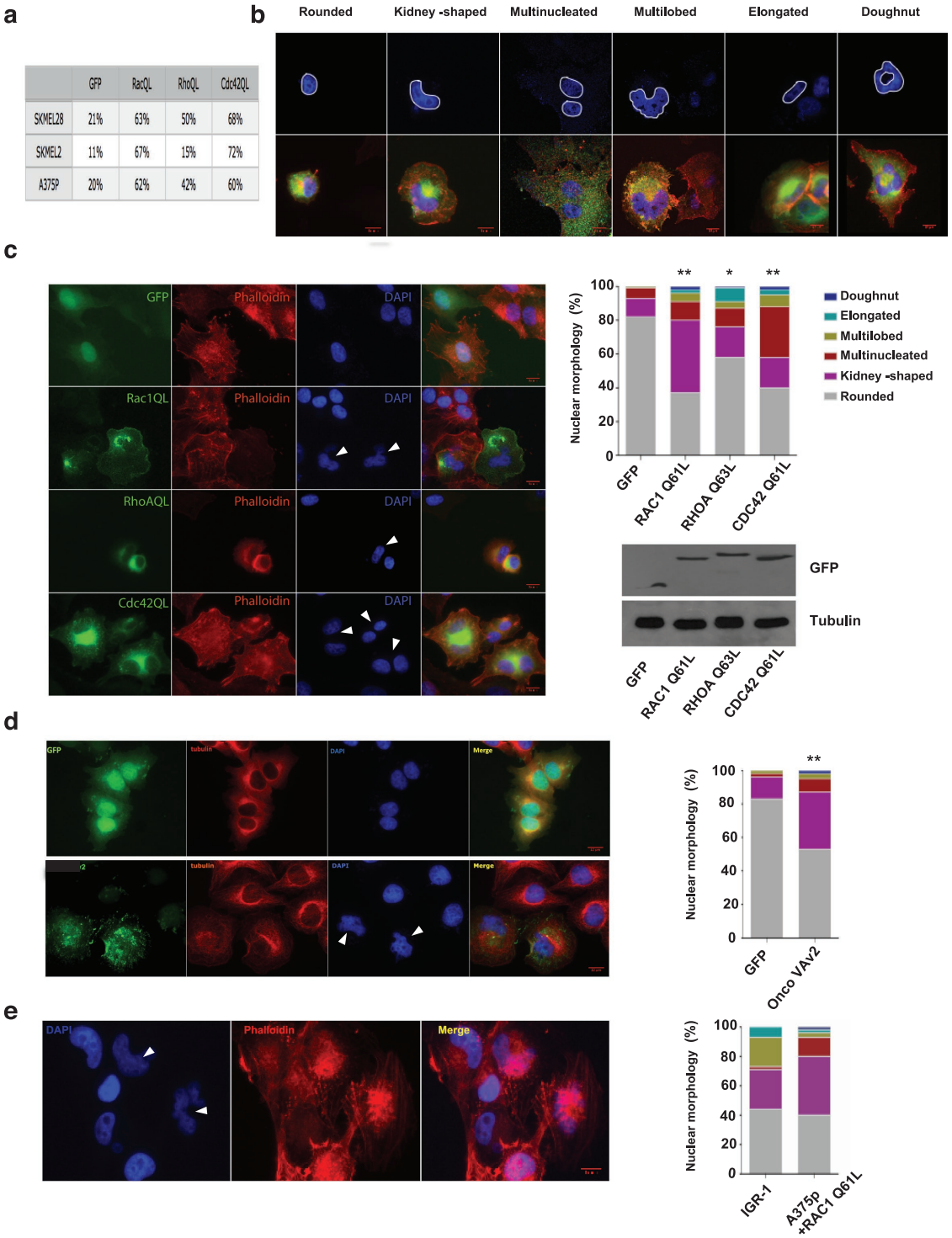

	GFP	RacQL	RhoQL	Cdc42QL
SKMEL28	21%	63%	50%	68%
SKMEL2	11%	67%	15%	72%
A375P	20%	62%	42%	60%

FIGURE 1: RHO GTPases induce nuclear morphology alterations in melanoma cells. (a) Percentage of nuclei affected by the overexpressed RHO GTPases in different melanoma cell lines. (b) Classification of the nuclear morphology resulting from the overexpression of the GTPases. Fluorescence microscopy images showing the different nuclear shapes elicited by RHO GTPases in A375p cells. (c) Quantification of nuclear morphological alterations in A375p cells transfected with activated RHO GTPases (1 µg each) and analyzed by fluorescence microscopy. Left panel: Representative immunofluorescence images of cells transfected with GFP (control), RAC1QL, RHOAQL, and CDC42QL. Right panel: Quantification of nuclei morphologies. Bottom panel: immunoblot showing the expression of the GTPases. (d) Vav2 overexpression increases the number of aberrant nuclei in A375p cells. (e) Distribution of altered nuclear morphologies in IGR-1 cells. Left panel: Representative fluorescence microscopy images of IGR1 cells shows high number of kidney-shaped nuclei. Blue, DAPI; red, Phalloidin. Right panel: quantification of the different nuclear morphologies in IGR1 cells compared with A375p cells expressing RAC1QL. Scale bar in all cases = 10 µm. Arrows show representative nuclear deformities. Asterisks mark the *p* values obtained relative to control ($n = 3$ independent experiments each performed in triplicate).

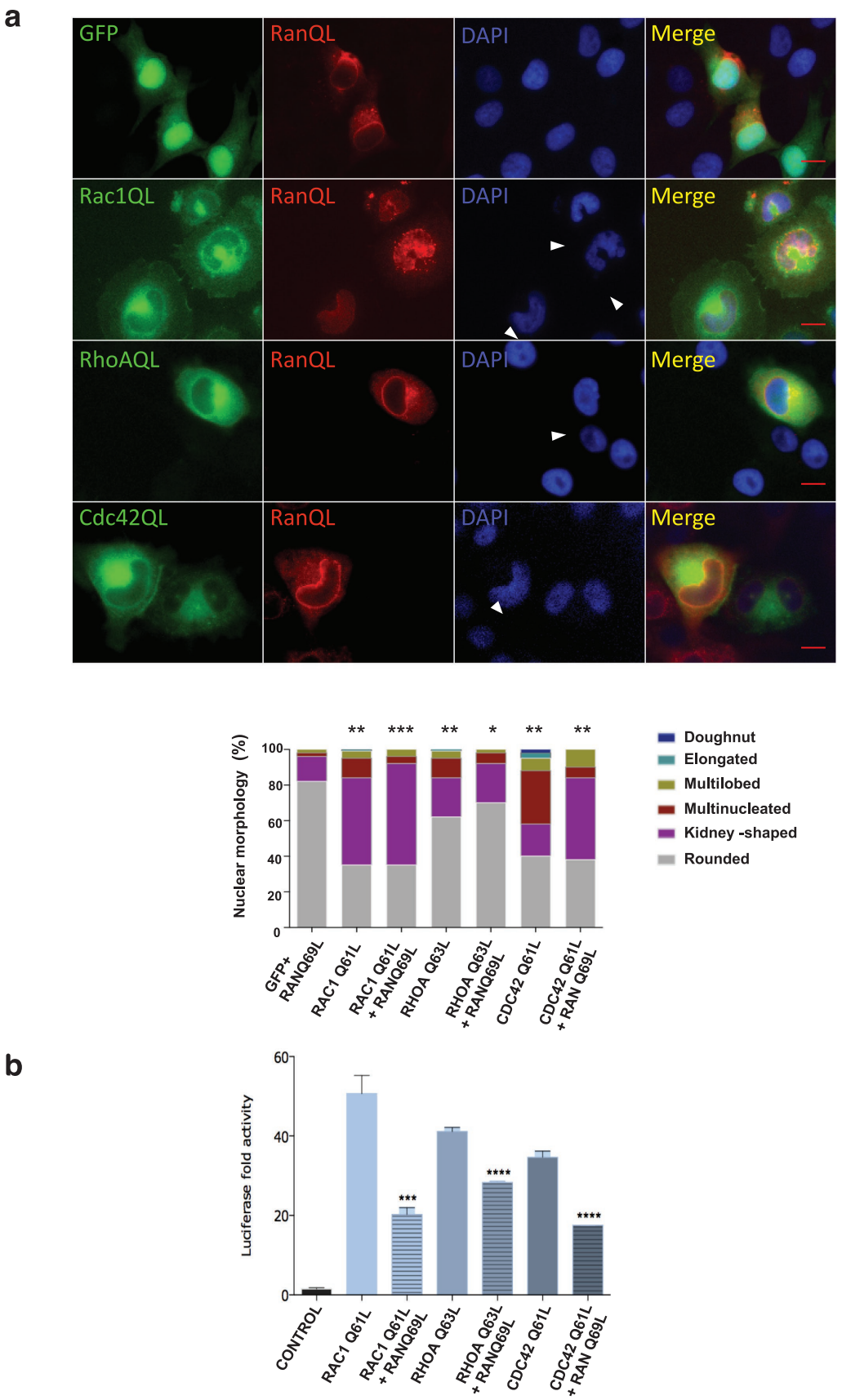

FIGURE 2: Alterations in nuclear morphology are independent of Rho GTPases-evoked gene expression. (a) Effect of the RHO GTPases on nuclear morphology in the presence of RanQL (1 μg each). Arrows show representative nuclear deformities. (b) Effects of RanQL overexpression on the transactivation of an SRE promoter by the activated GTPases. Data show average SEM from three independent experiments, *$p < 0.05$, **$p < 0.01$, ***$p < 0.005$, ****$p < 0.001$ by Student's *t* test.

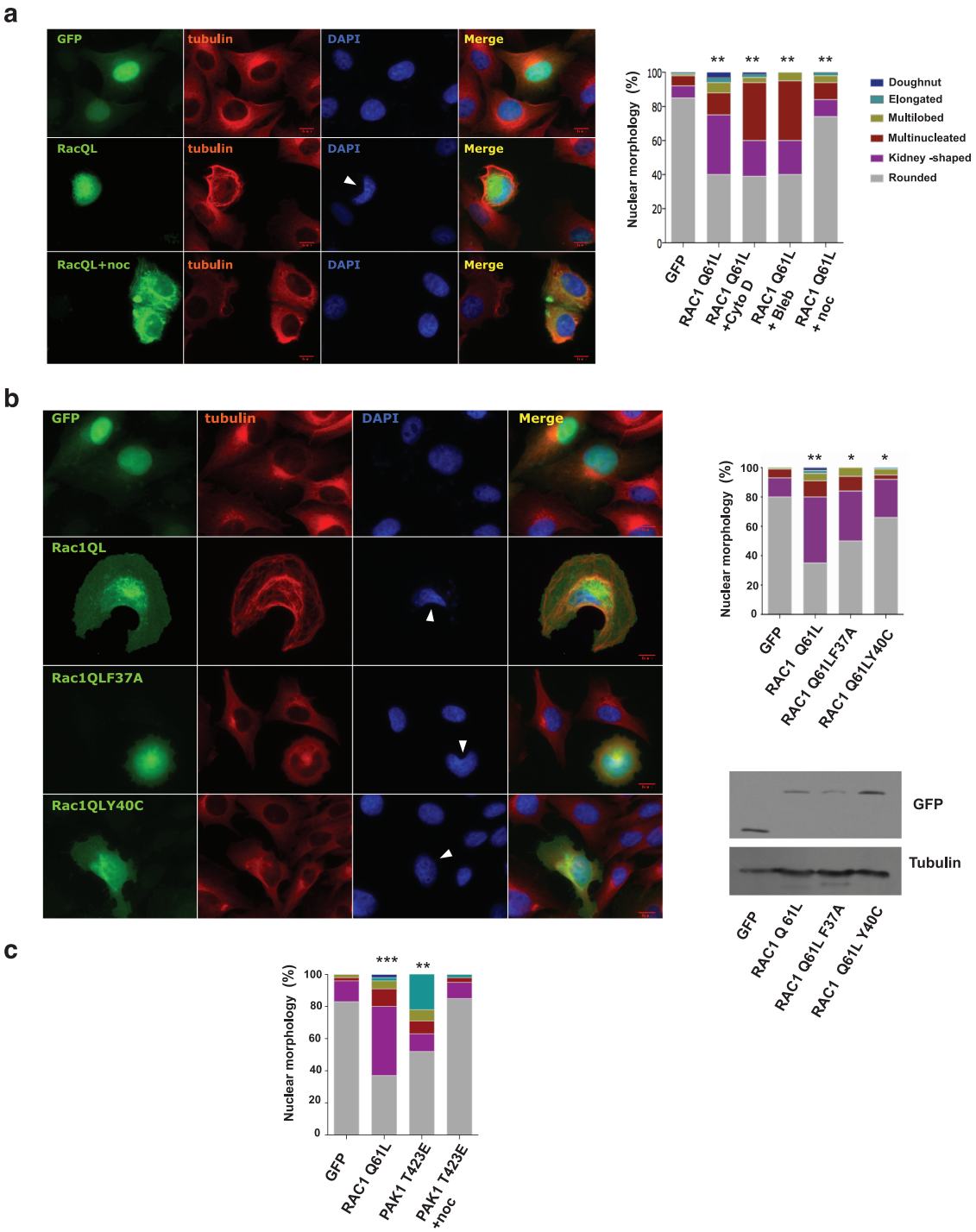

FIGURE 3: RAC1QL alters nuclear morphology through the tubulin cytoskeleton. (a) Effects of drugs acting on the tubulin and actin citoskeleton on RAC1QL-induced nuclear alterations in transfected A375p cells. Images and quantitations showing the effect of nocodazole (noc: 0.5 μM/24 h), Cytochalasin D (cytD: 1 μM/24 h), and blebbistatin (bleb: 5 μM/24 h). (b) Effects on nuclear morphology by the RAC1QL F37A and RAC1QL Y40C mutants (1 μg each). (c) Effects on nuclear morphology of a constitutively active PAK1 T423E mutant (1 μg each). Arrows show representative nuclear deformities. Data show average ± SEM from 3 independent experiments, *$p < 0.05$, **$p < 0.01$, ***$p < 0.005$ by Student's *t* test.

largely unaltered, although an increase in the number of binucleated cells was observed in both cases (Figure 3), which was not surprising, given that these treatments result in a failure in cytokinesis. We concluded that the effect of RAC1 activation on nuclear shape was mainly exerted through the microtubule cytoskeleton.

To further substantiate this point, we used several RAC1 mutants deficient for engaging different effector pathways; RAC1Q61L F37A activates effector proteins such as PAK1 or JNK; however, it does not induce alterations of the actin cytoskeleton (Joneson *et al.*, 1996; Joneson and Bar-Sagi, 1998). On the other hand, RAC1Q61L

Y40C induces membrane ruffling; therefore, it is capable of modifying the actin cytoskeleton (Joneson *et al.,* 1996; Lamarche *et al.,* 1996), but since it does not activate PAK1 it cannot inhibit stathmin, thereby preventing microtubule depolymerization (Wittmann *et al.,* 2004). When compared with RAC1Q61L, both mutants induced nuclear pleomorphism to a lesser extent, particularly in the case of the Y40C mutant (Figure 3b), incapable of preventing microtubule depolymerization, consistent with the results obtained in the previous experiment using nocodazole. Furthermore, overexpression of a constitutively active form of PAK1, PAK1 T423E (Zenke *et al.,* 1999), was sufficient to induce marked alterations on nuclear shape. However, the nuclear morphologies yielded by PAK activation differed considerably from those elicited by active RAC1, with elongated nuclei being the most abundant deformation (Figure 3c). As in the case of RAC1, nocodazole treatment completely abolished the nuclear alterations evoked by active PAK1 (Figure 3c), confirming microtubules as mediators of nuclear shape control by RAC1 and PAK1.

Overall, we can conclude that RAC1 activation can induce nuclear alterations mainly through its ability to regulate microtubule polymerization. However, there seems to be additional RAC1-regulated mechanisms affecting nuclear shape, since tampering with the actin cytoskeleton also impacts on nuclear morphology and PAK1 activation alone yields different patterns of nuclear deformation.

LINC complex proteins mediate in the regulation of nuclear morphology by RAC1

Since the LINC complex constitutes the physical connection between the cytoskeleton and the nucleus (Lombardi and Lammerding, 2011), we asked whether the effect of RAC1 on nuclear morphology was transmitted through this complex. To this end, we utilized mutant forms of SUN and KASH proteins, which act as dominant inhibitory mutants when overexpressed. These mutant proteins interfere in the interactions of endogenous components of the LINC complex, resulting in a drop on the concentration of nesprins in the outer nuclear membrane, thereby severing the connections with the cytoskeleton (Crisp *et al.,* 2006; Stewart-Hutchinson *et al.,* 2008). Indeed, the expression of these dominant-negative proteins markedly decreased the percentage of anomalous nuclei when cotransfected with RAC1QL (Figure 4a).

To further substantiate this point, we analyzed how the disruption of the LINC complex affected the dynamics of the nuclear changes induced by active RAC1. To analyze the rate of change in nuclear morphology, captions of the nuclei were taken every 10 min during a 3-h period, and three parameters were evaluated: nuclear area, perimeter, and roundness. We found that cells expressing RAC1QL showed a high nuclear morphology alteration rate with respect to the three parameters measured, as opposed to control cells where changes were hardly detectable. Noticeably, expression of KASH DN markedly reduced the dynamics of nuclear alterations, particularly in the case of nuclear roundness (Figure 4b). We concluded that the breakdown of the LINC complex largely prevents nuclear morphology changes induced by the activation of RAC1.

RAC1QL induces LINC-dependent invasion and intravasation of melanoma cells

RHO GTPases are functionally connected to cellular migration and the invasive capacity of cells (Schmitz, Govek *et al.,* 2000; Lawson and Ridley, 2018). Therefore, we hypothesized that nuclear deformation, as induced by RHO GTPases, could provide advantages in invasive processes by facilitating cell passage through narrow spaces, as the nucleus is the largest and most rigid organelle, thereby posing the limiting factor in this respect (Wolf *et al.,* 2013). Thus, we analyzed if the degree of nuclear deformation correlated with greater invasive capacity by using a matrigel transwell migration assay. We found that A375p cells overexpressing active RHO GTPases, particularly RAC1QL, invaded in greater numbers with respect to control cells (Figure 5a, Supplemental Figure S3, and Supplemental Video).

Based on these results, we analyzed invasion in vivo by using the chick embryo chorioallantoid membrane (CAM) model (Deryugina and Quigley, 2008). In this context, we found that the expression of the constitutively active GTPase in A375p melanoma cells did not result in significant variations with respect to the growth rate of the primary tumor (Figure 5b). Contrarily, it could be observed that the overexpression of RAC1Q61L conferred A375p cells with a remarkable ability to intravasate (Figure 5b).

Finally, we studied whether the integrity of the LINC complex affected the invasion process, as induced by RAC1QL. Overexpression of the KASH DN dominant-negative mutant had no effect on tumor growth, but dramatically reduced the ability of RAC1Q61L-expressing cells to intravasate (Figure 5c). This result was further confirmed using the intramesodermal chicken embryo model to quantify cell escape from the primary microtumors, linking cell motility and invasion to tumor cell intravasation (Casar *et al.,* 2014). Within 5 d after microinjections, tumor cells could be observed escaping from well-formed microtumors and invading the surrounding stroma. It was observed that the number of RAC1QL-expressing cells escaping the tumor was markedly reduced when expressing KASH DN (Figure 5d), thereby demonstrating that the connection of the cytoskeleton with the nucleus through the LINC complex is essential for melanoma cell intravasation.

DISCUSSION

Herein we demonstrate that activated RHO GTPases, particularly RAC1, induce nuclear shape alterations to regulate the migratory and invasive properties of melanoma cells. We show that such alterations are not a consequence of gene expression-regulated events, but rather mechanically evoked via the cytoskeleton, primarily the tubulin cytoskeleton, in connection with the LINC complex.

Our results are quite in line with previous data showing that microtubules are responsible for maintaining the nuclear structure (Tremblay *et al.,* 2013) and can exert forces on the nucleus capable of changing its appearance (Hampoelz *et al.,* 2011; Zwerger *et al.,* 2011). Likewise, the participation of RHO GTPases in nuclear shape control via the actin cytoskeleton has been previously proposed (Khatau *et al.,* 2009; Versaevel *et al.,* 2012). While there is ample evidence on the regulation of the tubulin cytoskeleton by RHO GTPases (Bartolini *et al.,* 2008; Pleines *et al.,* 2013; Tivodar *et al.,* 2015), it is somehow surprising that the control of nuclear morphology in melanoma cells by RHO GTPases is exerted primarily through microtubules rather than through its main effector, the actin cytoskeleton. Intriguingly, RAC1 can also induce nuclear alterations from within the nucleus through nuclear actin (Navarro-Lerida *et al.,* 2015). In this respect, our data suggest that RAC1 regulates nuclear shape through its effector PAK1. This can be envisioned by the fact that nuclear deformation is impaired to a large extent in a RAC1QL mutant defective for activating PAK1 and also as a constitutively active PAK1 can readily induce aberrant nuclei. Indeed, PAK1 is known to regulate tubulin polymerization through the phosphorylation of stathmin (Wittmann *et al.,* 2004), serving as the mechanistic link to connect RAC1 activation to the regulation of the tubulin cytoskeleton. However, our results demonstrate that the patterns of nuclear alterations elicited by RAC1 and PAK1 are different, hinting that it is

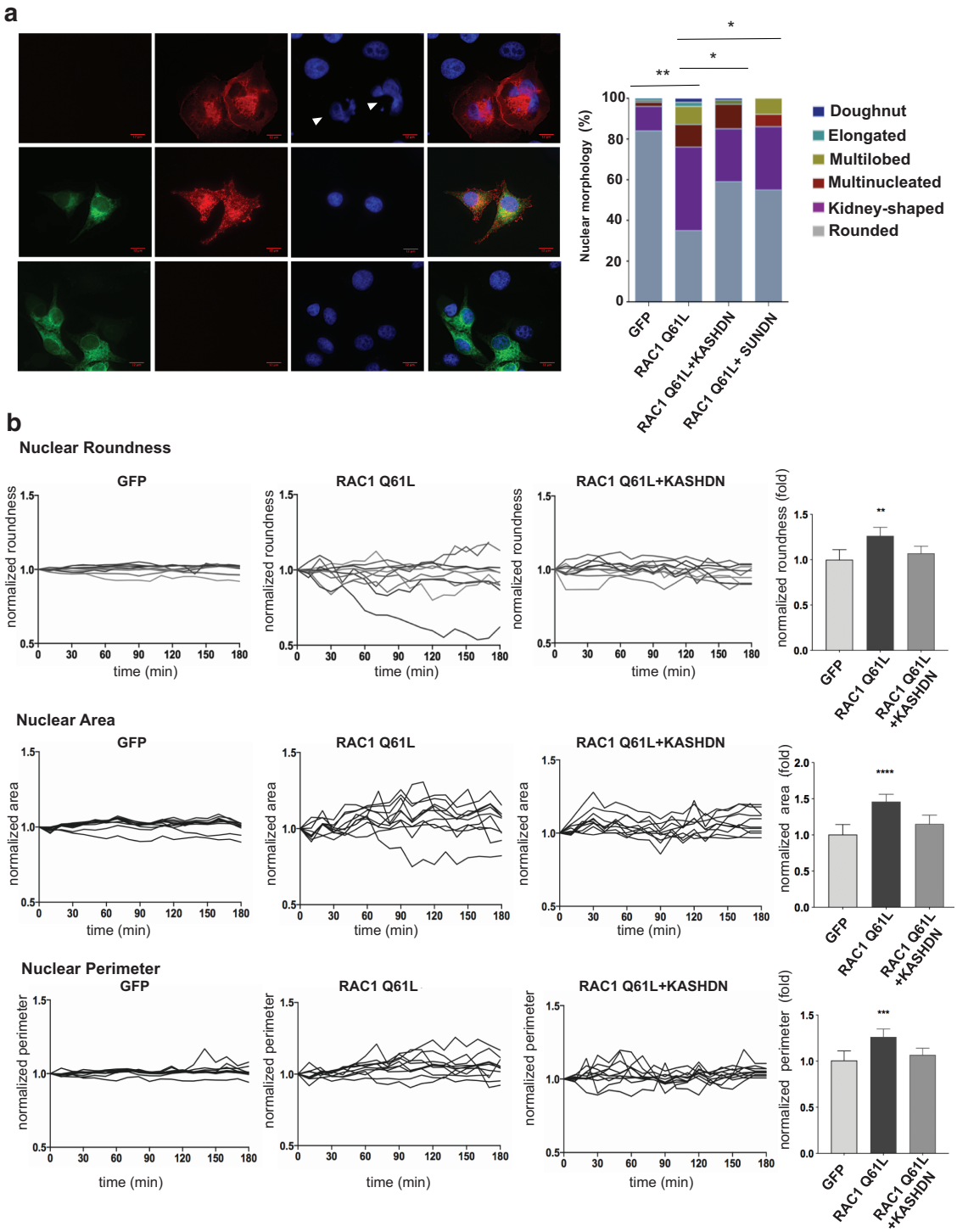

FIGURE 4: The LINC complex mediates in the regulation of nuclear morphology by RAC1. (a) Expression of SUN and KASH dominant-negative mutants (1 μg each) affects the proportion of anomalous nuclei induced by RAC1QL. (b) Effects of the expression of KASH dominant-negative mutant on the dynamics of nuclear alteration parameters: nuclear area, perimeter, and roundness monitored by time-lapse microscopy in A375p cells. For each condition, 10 nuclei were analyzed during 3 h. Quantitation of nuclear alteration parameters showing changes relative to the control (right panels). Asterisks mark the *p* values obtained from three independent experiments, each performed in triplicate. Data show average ± SEM, $*p < 0.05$, $**p < 0.01$, $***p < 0.005$, $****p < 0.001$ by Student's *t* test.

unlikely that PAK1 would be the only RAC1 effector involved in the regulation of nuclear morphology.

It has been demonstrated that preventing the nucleo–cytoplasmic connection by disrupting the LINC complex has a negative effect on nuclear dynamics (Khatau *et al.*, 2009; Petrie *et al.* 2014). In line with these results, we have observed that disrupting the cytoskeleton–LINC complex connection completely reverts nuclear deformation as induced by active RAC1. Furthermore, the LINC

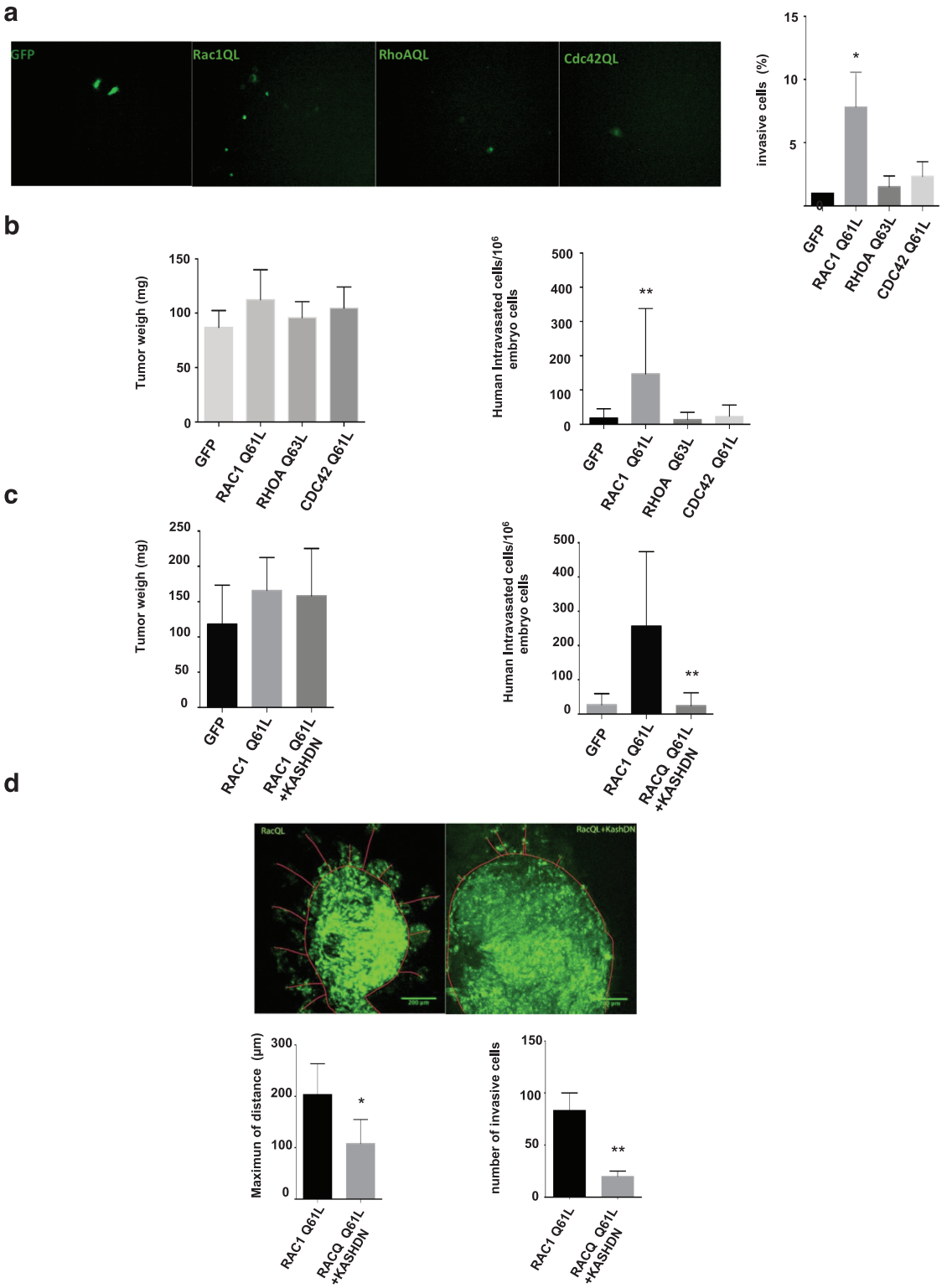

FIGURE 5: Activated RAC1 induces LINC-dependent invasion and intravasation of melanoma cells. (a) Representative results from a transwell migration assay of A375p cells expressing the different activated RHO GTPases. (b) Effects of RAC1QL expression in A375p on tumor growth (left panel) and intravasation (right panel), using the chick embryo CAM model. (c) Effects of the expression of KASH dominant-negative mutant on tumor growth and intravasation induced by RAC1QL (1 µg each) in A375p cells xenografted in the chick embryo CAM model. (d) Ex ovo analysis of cells escaping from the microtumor using the chicken embryo intramesodermal model. In all cases, graphs show mean value ± SD. NS, nonsignificant, $*P < 0.05$, $**P < 0.01$ by Student's *t*-test.

complex is critical for the transmission of force between the cytoplasm and the nucleus, and breaking the interaction between these two compartments leads to failures in the position of the nucleus, resulting in a diminished cellular migration (Lombardi *et al.,* 2011). In agreement with this notion, we demonstrate that the invasive properties of melanoma cells harboring active RAC1 are markedly impaired when the cytoskeleton–LINC complex connection is disrupted by the use of KASH- and SUN-dominant inhibitory mutants.

Nuclear atypia, including invaginations of the nuclear envelope, lobulated, and kidney-shaped nuclei, among other deformities, is frequent in many types of cancer (de Las Heras *et al.,* 2013). In this study, we also analyzed the implications of nuclear deformation in biological processes relevant for tumorigenesis, such as invasion. We have shown that the expression of activated RAC1 enhances invasive processes in melanoma cells, both in vitro using the transwell assays and in vivo with the chick embryo model, quite in line with previous reports (Lorentzen *et al.,* 2011). However, we have demonstrated that the disruption of the LINC complex, preventing nuclear deformation, forestalls melanoma cells dissemination. Thus, it is tempting to speculate that the ability of tumor cells to deform the nucleus via RAC1 activation would confer them with enhanced invasive abilities. Indeed, many human tumors are characterized by overexpression or hyperactivation of RAC1 (Karlsson *et al.,* 2009), while in others, such as those harboring RAS oncogenes, cross-talk with RHO GTPases via activation of exchange factors such as TIAM (Lambert *et al.,* 2002) would facilitate this process. Thus, interfering with RHO GTPases ability for nuclear deformation could be a valid strategy for preventing metastatic dissemination.

MATERIALS AND METHODS

Cell culture and transfection

A375p (Cat #CRL-3224, RRID: CVCL_6233, ATCC, Manassas, VA) and IGR-1 (CLS Cat #300219/p483_IGR-1, RRID:CVCL_1303) cells were obtained from the American Type Culture Collection and grown in DMEM supplemented with 10% fetal bovine serum (FBS; Life Technologies, Waltham, MA). Mycoplasma testing was undertaken every month using commercial Mycoplasma testing kits (Biotools, Madrid, Spain). All cell lines used in this work have been authenticated every 12 mo by short tandem repeat profiles using the Applied Biosystems Identifier kit in the Genomic Facility at IBBTEC (Institute of Biomedicine and Biotechnology of Cantabria). The plasmids pEGFP, pEGFP RAC1Q61L, pEGFP RAC1N17, pEGFP RHOA Q63L, pEGFP CDC42 Q61L, pEGFP RAC Q61L F37A, pEGFP RAC Q61L Y40C, pEGFP OncoVAv2, and pSRE luc were provided by Xosé R. Bustelo. pEGFP KASH DN was provided by Cathy Shanahan and pCDHEF1-SUNDN by Sue Shackleton. pCEFL HA RAC N17, pCEFL HA RHOA N17, and pCEFL HA CDC42 N17 plasmids were generated by PCR and cloned into pCEFL HA vector. Where applicable, stable lines cells were generated by transfection with Lipofectamine (Invitrogen, NY) or FuGene following manufacturer's instructions and selected with 750 µg/ml G418 (Invitrogen) where necessary. For biochemical analyses, subconfluent cells were transfected with Lipofectamine 2000 and 3000 (Invitrogen). For immunofluorescence studies, cells were transfected with FuGENE transfection reagent (Roche, Basel, Switzerland).

Immunoblotting

Cell lysates were prepared in lysis buffer supplemented with protease and phosphatase inhibitor cocktail (Thermo Scientific). Equal amounts of protein, as measured by BCA protein assay, were resolved in 4–12% Bis-Tris gradient gels and transferred electrophoretically on a nitrocellulose membrane. Membranes were blocked for 1 h at room temperature in 4% bovine serum albumin (BSA) in Tris-buffered saline (TBS)T before being incubated overnight at 4°C with the primary antibodies. All primary antibodies were diluted in 4% BSA. After three washes of 5 min in TBST, horseradish peroxidase–conjugated secondary antibodies (Bio-Rad Laboratories, Hercules, CA) were diluted 1:5000 in 0.4% BSA in TBST and incubated for 1 h at room temperature. After another three washes in TBST, detection of the signal was achieved by incubating with ECL chemoluminiscence detection (GE Healthcare, Little Chalfont, Buckinghamshire, UK) and exposing it on autoradiography films from Denville Scientific (Metuchen, NJ).

The primary antibodies used were mouse monoclonal anti-GFP (1:2000 dilution, Sigma-Aldrich Cat #SAB4200681, RRID:AB_2827519), anti-tubulin (1:5000 dilution, Sigma-Aldrich Cat #T8328, RRID:AB_1844090), and mouse monoclonal anti-HA (1:1000 dilution, Sigma-Aldrich Cat #H6533, RRID:AB_439705).

cDNA-synthesis and qRT-PCR analysis

cDNA was synthesized using iScript cDNA Synthesis Kit (Bio-Rad) using 1 µg of isolated RNA per reaction by Speedtools Total RNA extraction Kit (Biotools, Madrid, Spain). Reverse transcription was performed in an Applied Biosystems Thermal Cycler with the following settings: 25°C for 5 min, 46°C for 20 min, and 95°C for 1 min.

qPCR reactions were performed in triplicate using SYBR Select Master Mix (Applied Biosystems) in a StepOnePlus Real-Time PCR System (Thermo Fisher Scientific) with standard conditions: 50°C for 2 min (UDG activation) and 95°C for 2 min (Polymerase activation) followed by 40 cycles of 95°C for 15 s (denaturation) and 60°C for 1 min (annealing and elongation). Target genes were normalized to *S14* expression. Human primer sequences were the following: TCACCTACCAGGTGTCGGAGTC(*Srf*_f), GTGCTGTTTGGATGGTGGAGGT (*Srf*_r), CACCATTGGCAATGAGCGGTTC (*Actg1*_f), AGGTCTTTGCGGATGTCCACGT (*Actg1*_r), GGAAAAGGCAGCTCACTGAAGC (*Cyr61*_f), GGAGATACCAGTTCCACAGGTC (*Cyr61*_r), GGTGGACATTGGCGTCAAGTAC (*Cnn2*_f), GGGTCATAGAGATGCCTTCTCG (*Cnn2*_r), TATCACCGCCCTACACATCA(*S14*_f), and GGGGTGACATCCTCAATCC (*S14*_r).

Matrigel invasion assay

In Matrigel invasion assays, the upper side of membranes (8 µm pore Transwell, Fisher Scientific) was precoated with 2 µg Matrigel (BD Biosciences), and 10% FBS-DMEM was added as a chemoattractant in the lower chamber; 1×10^5 A375p cells were plated in 150 µl of SF-DMEM in the upper chamber. Two hours after seeding the cells, real-time invasion was analyzed by confocal microscopy (TCS SP-5, Leica) for 24 h taking pictures every 30 min. Hoechst 33258 (0.2 µg/µl, Thermo Fisher Scientific) was added to dye the nuclei. Images were processed and analyzed using Fiji ImageJ (National Institutes of Health [NIH], Bethesda, MD). Following 48 h incubation, the invaded cells were fixed and analyzed by fluorescence microscopy and counted after crystal violet staining.

Time-lapse immunofluorescence

Cells were grown on polylysine-coated, glass-bottom dishes and transiently cotransfected with indicated plasmids. Cells were placed into a microscope chamber and treated with agonists. Confocal images (512 × 512 pixels; 0.15 pixel size) were acquired at 37°C in a TCS SP-5 confocal microscope (Leica) with a 40×, 1.25 NA oil objective, a 1 Airy pinhole, and 200 Hz speed. Images were captured every 2 min. Cells were excited with 405-, 458-, and 543-nm

laser lines. Images are presented after digital adjustment of brightness and contrast to maximize signal. Images were processed and analyzed using Fiji ImageJ (NIH, Bethesda, MD).

Confocal immunofluorescence

Cultured cells were washed twice in PBS, fixed with ice-cold methanol for 5 min, and washed with PBS. They were rinsed in PBS–0.05% Tween 20 (Sigma, Saint Louis, MO), incubated for 2 h with the primary antibodies washed, and incubated for 1 h with the appropriate secondary antibodies conjugated to FITC or Texas Red. Coverslips were mounted in VECTASHIELD-DAPI (Vector Laboratories, Burlingame, CA) and sealed. Confocal microscopy was performed with an LSM510 microscope (Carl Zeiss, Thornwood, NY) by using excitation wavelengths of 488 nm (for FITC) and 543 nm (for Texas Red). The images were then processed and analyzed using Fiji ImageJ (NIH, Bethesda, MD).

Dual luciferase reporter assay

A Renilla-luciferase reporter assay was carried out to examine the effect of ERα and CBP knockdown on pS2 promoter activity. A total of 5×10^4 cells were seeded on a 24-well plate in antibiotic free media for 24 h. Cells were transfected with 12.5 ng Renilla vector (used as an internal control) pRL Null Renilla and pSRE luc. After 24 h of transfection, cells were harvested for 16 h, stimulated with EGF (100 ng/ml for 2 h), and lysed. Luciferase activity was tested using the Dual-Luciferase Reporter Assay System (Promega) as instructed by the manufacturer, and luciferase detection was measured on Monolight 3010 Luminometer (Promega, Madison, WI). Experiments were carried out in duplicate in three independent experiments.

Intramesodermal microtumor model for tumor cell escape and invasion in vivo

Escape from microtumors and invasion of cells in vivo was carried out in live chick embryos (Granja Gibert, Tarragona, Spain) as described (Casar *et al.,* 2014). Briefly, A375p cells were labeled with CellTracker Green CMFDA (Molecular Probes, Invitrogen) and injected into the mesoderm layer of the CAM of 9-day-old chicken embryos. Five to seven small boluses of tumor cells (3–5 µl) were injected directly into the CAM mesoderm of chick embryos developing ex ovo. At day 5, portions of the CAM containing microtumors were excised and immediately imaged using a Carl Zeiss Axio Imager microscope. Quantification of tumor cell escape and invasion was performed using ImageJ software (NIH, Bethesda, MD). The mean number of the cells escaped and the mean of invasion distances from the tumor-CAM border were determined for each microtumor. A total of 12 to 15 individual microtumors from five to eight embryos was analyzed for each variable in three independent experiments.

The chick embryo model for tumor cell dissemination and metastasis

Analysis of spontaneous intravasation and dissemination of A375p cells carried out in chick embryos was as described (Casar *et al.,* 2012). Briefly, chick embryos (Granja Gibert, Tarragona, Spain) were allowed to develop in a humidified 37°C incubator. After 10 d of incubation, 1×10^6 A375p cells were grafted through a window in the eggshell onto the CAM of each embryo. On day 7, primary tumors were removed and weighed, and portions of the distal CAM and livers were excised and analyzed by *Alu*-qPCR to determine actual numbers of human cells in the chicken tissue, essentially as described (Casar *et al.,* 2012).

Statistical analyses

Throughout, graphed data are expressed as mean ± SEM. All statistical analyses were carried out using GraphPad Prism software (GraphPad Software, San Diego, CA). The number of replicates and the statistical tests used in each case are indicated in the figure legends. In all cases, $*p < 0.05$, $**p < 0.01$, and $***p < 0.005$. For experiments involving cultured cells, unless otherwise stated, values are expressed as means ± SEM of three independent experiments; *P* values were calculated with the two-tailed Student's *t* test, 95% significance, and two-way ANOVA. To test for the homogeneity of variances, we ran a previous *F* test of equality of variances. Significance was assessed using parametric or nonparametric tests as appropriate.

ACKNOWLEDGMENTS

B.C.'s laboratory is supported by a Retos Jóvenes Investigadores grant SAF2015-73364-JIN Ministerio de Ciencia, Innovación y Universidades (MICIU/AEI/FEDER, UE), a PIE grant from Consejo Superior de Investigaciones Científicas (CSIC)—MCIU, and the Ramón y Cajal Research Program (MICIU, RYC2018-024004-I). P.C is supported by grant SAF-2015 63638R (MINECO/FEDER, UE); by Red Temática de Investigación Cooperativa sobre el Cáncer (RTICC), RD/12/0036/0033, and by Asociación Española Contra el Cáncer (AECC) grant GCB141423113. X.R.B. is supported by grants from the Castilla-León Government (BIO/SA01/15, CSI049U16), MINECO (SAF2015-64556-R, RD12/0036/0002), Worldwide Cancer Research (14-1248), Ramón Areces Foundation, and AECC (GC16173472GARC). Spanish funding to B.C., P.C., and X.R.B. is partially supported by the European Regional Development Fund. We thank Alicia Noriega for technician support.

REFERENCES

Abe K, Rossman KL, Liu B, Ritola KD, Chiang D, Campbell SL, Burridge K, Der CJ (2000). Vav2 is an activator of Cdc42, Rac1, and RhoA. J Biol Chem 275, 10141–10149.

Abreu-Blanco MT, Verboon JM, Parkhurst SM (2014). Coordination of Rho family GTPase activities to orchestrate cytoskeleton responses during cell wound repair. Curr Biol 24, 144–155.

Atilla-Gokcumen GE, Castoreno AB, Sasse S, Eggert US (2010). Making the cut: the chemical biology of cytokinesis. ACS Chem Biol 5, 79–90.

Bartolini F, Moseley JB, Schmoranzer J, Cassimeris L, Goode BL, Gundersen GG (2008). The formin mDia2 stabilizes microtubules independently of its actin nucleation activity. J Cell Biol 181, 523–536.

Bid HK, Roberts RD, Manchanda PK, Houghton PJ (2013). RAC1: an emerging therapeutic option for targeting cancer angiogenesis and metastasis. Mol Cancer Ther 12, 1925–1934.

Busche S, Descot A, Julien S, Genth H, Posern G (2008). Epithelial cell-cell contacts regulate SRF-mediated transcription via Rac-actin-MAL signalling. J Cell Sci 121(Pt 7), 1025–1035.

Casar B, He Y, Iconomou M, Hooper JD, Quigley JP, Deryugina EI (2012). Blocking of CDCP1 cleavage in vivo prevents Akt-dependent survival and inhibits metastatic colonization through PARP1-mediated apoptosis of cancer cells. Oncogene 31, 3924–3938.

Casar B, Rimann I, Kato H, Shattil SJ, Quigley JP, Deryugina EI (2014). In vivo cleaved CDCP1 promotes early tumor dissemination via complexing with activated beta1 integrin and induction of FAK/PI3K/Akt motility signaling. Oncogene 33, 255–268.

Chang W, Antoku S, Ostlund C, Worman HJ, Gundersen GG (2015). Linker of nucleoskeleton and cytoskeleton (LINC) complex-mediated actin-dependent nuclear positioning orients centrosomes in migrating myoblasts. Nucleus 6, 77–88.

Chen CY, Chi YH, Mutalif RA, Starost MF, Myers TG, Anderson SA, Stewart CL, Jeang KT (2012). Accumulation of the inner nuclear envelope protein Sun1 is pathogenic in progeric and dystrophic laminopathies. Cell 149, 565–577.

Cook DR, Rossman KL, Der CJ (2014). Rho guanine nucleotide exchange factors: regulators of Rho GTPase activity in development and disease. Oncogene 33, 4021–4035.

Crisp M, Liu Q, Roux K, Rattner JB, Shanahan C, Burke B, Stahl PD, Hodzic D (2006). Coupling of the nucleus and cytoplasm: role of the LINC complex. J Cell Biol 172, 41–53.
Croft DR, Olson MF (2011). Transcriptional regulation of Rho GTPase signaling. Transcription 2, 211–215.
Davis MJ, Ha BH, Holman EC, Halaban R, Schlessinger J, Boggon TJ (2013). RAC1P29S is a spontaneously activating cancer-associated GTPase. Proc Natl Acad Sci USA 110, 912–917.
de Las Heras JI, Batrakou DG, Schirmer EC (2013). Cancer biology and the nuclear envelope: a convoluted relationship. Semin Cancer Biol 23, 125–137.
Deryugina EI, Quigley JP (2008). Chick embryo chorioallantoic membrane model systems to study and visualize human tumor cell metastasis. Histochem Cell Biol 130, 1119–1130.
Erhardt K, Silfversward C, Auer G (1989). Nuclear DNA content and nuclear atypia. Relation to survival in patients with breast adenocarcinoma and serious ovarian tumors. Anticancer Res 9, 1325–1330.
Hall A, Nobes CD (2000). Rho GTPases: molecular switches that control the organization and dynamics of the actin cytoskeleton. Philos Trans R Soc Lond B Biol Sci 355, 965–970.
Hampoelz B, Azou-Gros Y, Fabre R, Markova O, Puech PH, Lecuit T (2011). Microtubule-induced nuclear envelope fluctuations control chromatin dynamics in Drosophila embryos. Development 138, 3377–3386.
Joneson T, Bar-Sagi D (1998). A Rac1 effector site controlling mitogenesis through superoxide production. J Biol Chem 273, 17991–17994.
Joneson T, McDonough M, Bar-Sagi D, Van Aelst L (1996). RAC regulation of actin polymerization and proliferation by a pathway distinct from Jun kinase. Science 274, 1374–1376.
Karlsson R, Pedersen ED, Wang Z, Brakebusch C (2009). Rho GTPase function in tumorigenesis. Biochim Biophys Acta 1796, 91–98.
Kazanietz MG, Caloca MJ (2017). The Rac GTPase in Cancer: From Old Concepts to New Paradigms. Cancer Res 77, 5445–5451.
Khatau SB, Hale CM, Stewart-Hutchinson PJ, Patel MS, Stewart CL, Searson PC, Hodzic D, Wirtz D (2009). A perinuclear actin cap regulates nuclear shape. Proc Natl Acad Sci USA 106, 19017–19022.
Krauthammer M, Kong Y, Ha BH, Evans P, Bacchiocchi A, McCusker JP, Cheng E, Davis MJ, Goh G, Choi M, *et al.* (2012). Exome sequencing identifies recurrent somatic RAC1 mutations in melanoma. Nat Genet 44, 1006–1014.
Lamarche N, Tapon N, Stowers L, Burbelo PD, Aspenstrom P, Bridges T, Chant J, Hall A (1996). Rac and Cdc42 induce actin polymerization and G1 cell cycle progression independently of p65PAK and the JNK/SAPK MAP kinase cascade. Cell 87, 519–529.
Lambert JM, Lambert QT, Reuther GW, Malliri A, Siderovski DP, Sondek J, Collard JG, Der CJ (2002). Tiam1 mediates Ras activation of Rac by a PI(3)K-independent mechanism. Nat Cell Biol 4, 621–625.
Lawson CD, Ridley AJ (2018). Rho GTPase signaling complexes in cell migration and invasion. J Cell Biol 217, 447–457.
Lindsay CR, Lawn S, Campbell AD, Faller WJ, Rambow F, Mort RL, Timpson P, Li A, Cammareri P, Ridgway RA, *et al.* (2011). P-Rex1 is required for efficient melanoblast migration and melanoma metastasis. Nat Commun 2, 555.
Lionarons DA, Hancock DC, Rana S, East P, Moore C, Murillo MM, Carvalho J, Spencer-Dene B, Herbert E, Stamp G, *et al.* (2019). RAC1^{P29S} Induces a mesenchymal phenotypic switch via serum response factor to promote melanoma development and therapy resistance. Cancer Cell 36, 68–83.
Liu BP, Burridge K (2000). Vav2 activates Rac1, Cdc42, and RhoA downstream from growth factor receptors but not beta1 integrins. Mol Cell Biol 20, 7160–7169.
Lombardi ML, Jaalouk DE, Shanahan CM, Burke B, Roux KJ, Lammerding J (2011). The interaction between nesprins and sun proteins at the nuclear envelope is critical for force transmission between the nucleus and cytoskeleton. J Biol Chem 286, 26743–26753.
Lombardi ML, Lammerding J (2011). Keeping the LINC: the importance of nucleocytoskeletal coupling in intracellular force transmission and cellular function. Biochem Soc Trans 39, 1729–1734.
Lorentzen A, Bamber J, Sadok A, Elson-Schwab I, Marshall CJ (2011). An ezrin-rich, rigid uropod-like structure directs movement of amoeboid blebbing cells. J Cell Sci 124(Pt 8), 1256–1267.
Luxton GW, Starr DA (2014). KASHing up with the nucleus: novel functional roles of KASH proteins at the cytoplasmic surface of the nucleus. Curr Opin Cell Biol 28, 69–75.
Maldonado MDM, Dharmawardhane S (2018). Targeting Rac and Cdc42 GTPases in Cancer. Cancer Res 78, 3101–3111.
Moshfegh Y, Bravo-Cordero JJ, Miskolci V, Condeelis J, Hodgson L (2014). A Trio-Rac1-Pak1 signalling axis drives invadopodia disassembly. Nat Cell Biol 16, 574–586.
Navarro-Lerida I, Pellinen T, Sanchez SA, Guadamillas MC, Wang Y, Mirtti T, Calvo E, Del Pozo MA (2015). Rac1 nucleocytoplasmic shuttling drives nuclear shape changes and tumor invasion. Dev Cell 32, 318–334.
Petrie RJ, Koo H, Yamada KM (2014). Generation of compartmentalized pressure by a nuclear piston governs cell motility in a 3D matrix. Science 345, 1062–1065.
Pleines I, Dutting S, Cherpokova D, Eckly A, Meyer I, Morowski M, Krohne G, Schulze H, Gachet C, Debili N, *et al.* (2013). Defective tubulin organization and proplatelet formation in murine megakaryocytes lacking Rac1 and Cdc42. Blood 122, 3178–3187.
Posern G, Treisman R (2006). Actin' together: serum response factor, its cofactors and the link to signal transduction. Trends Cell Biol 16, 588–596.
Schmitz AA, Govek EE, Bottner B, Van Aelst L (2000). Rho GTPases: signaling, migration, and invasion. Exp Cell Res 261, 1–12.
Starr DA, Hermann GJ, Malone CJ, Fixsen W, Priess JR, Horvitz HR, Han M (2001). unc-83 encodes a novel component of the nuclear envelope and is essential for proper nuclear migration. Development 128, 5039–5050.
Steggerda SM, Paschal BM (2002). Regulation of nuclear import and export by the GTPase Ran. Int Rev Cytol 217, 41–91.
Stewart-Hutchinson PJ, Hale CM, Wirtz D, Hodzic D (2008). Structural requirements for the assembly of LINC complexes and their function in cellular mechanical stiffness. Exp Cell Res 314, 1892–1905.
Straight AF, Cheung A, Limouze J, Chen I, Westwood NJ, Sellers JR, Mitchison TJ (2003). Dissecting temporal and spatial control of cytokinesis with a myosin II Inhibitor. Science 299, 1743–1747.
Takeshima N, Hirai Y, Hasumi K (1998). Prognostic validity of neoplastic cells with notable nuclear atypia in endometrial cancer. Obstet Gynecol 92, 119–123.
Tivodar S, Kalemaki K, Kounoupa Z, Vidaki M, Theodorakis K, Denaxa M, Kessaris N, de Curtis I, Pachnis V, Karagogeos D (2015). Rac-GTPases regulate microtubule stability and axon growth of cortical GABAergic nterneurons. Cereb Cortex 25, 2370–2382.
Tremblay D, Andrzejewski L, Leclerc A, Pelling AE (2013). Actin and microtubules play distinct roles in governing the anisotropic deformation of cell nuclei in response to substrate strain. Cytoskeleton 70, 837–848.
Vasquez RJ, Howell B, Yvon AM, Wadsworth P, Cassimeris L (1997). Nanomolar concentrations of nocodazole alter microtubule dynamic instability in vivo and in vitro. Mol Biol Cell 8, 973–985.
Vega FM, Ridley AJ (2008). Rho GTPases in cancer cell biology. FEBS Lett 582, 2093–2101.
Versaevel M, Grevesse T, Gabriele S (2012). Spatial coordination between cell and nuclear shape within micropatterned endothelial cells. Nat Commun 3, 671.
Wertheimer E, Gutierrez-Uzquiza A, Rosemblit C, Lopez-Haber C, Sosa MS, Kazanietz MG (2012). Rac signaling in breast cancer: a tale of GEFs and GAPs. Cell Signal 24, 353–362.
Wittmann T, Bokoch GM, Waterman-Storer CM (2004). Regulation of microtubule destabilizing activity of Op18/stathmin downstream of Rac1. J Biol Chem 279, 6196–6203.
Wolf K, Te Lindert M, Krause M, Alexander S, Te Riet J, Willis AL, Hoffman RM, Figdor CG, Weiss SJ, Friedl P (2013). Physical limits of cell migration: control by ECM space and nuclear deformation and tuning by proteolysis and traction force. J Cell Biol 201, 1069–1084.
Zenke FT, King CC, Bohl BP, Bokoch GM (1999). Identification of a central phosphorylation site in p21-activated kinase regulating autoinhibition and kinase activity. J Biol Chem 274, 32565–32573.
Zhang X, Lei K, Yuan X, Wu X, Zhuang Y, Xu T, Xu R, Han M (2009). SUN1/2 and Syne/Nesprin-1/2 complexes connect centrosome to the nucleus during neurogenesis and neuronal migration in mice. Neuron 64, 173–187.
Zwerger M, Ho CY, Lammerding J (2011). Nuclear mechanics in disease. Annu Rev Biomed Eng 13, 397–428.